Fluorescent Carbon Quantum Dot–Based Nano-Surfactants for Multifunctional Interfacial Modulation and Improved Oil Recovery in Low-Permeability Reservoirs

Zhang Guoqing[1,2], Yancheng Zheng[1,*], Xuejin Liu[1], Meichao Fan[1], Zhengyu Li[1], Hongyun Zhao[1]

[1] School of Chemical and Environmental Engineering, Yangtze University, No.1 Nanhuan Road, Jingzhou, Hubei 434023, China

[2] School of Energy and Petroleum industry, Kazakh-British Technical University, Almaty 050000, Kazakhstan

Supplementary Information

Table S1 Comparison of CQDs and other nanomaterials used as surfactants

Material	QY (%)	TEM	CMC (mM)	γcmc ($mN \cdot m^{-1}$)	Contact angle	Corrosion inhibition	Antibiotic activity	EOR	Ref
PHA-CDs, PCA-CDs, PDA-CDs	/	1.9-18.8nm	/	/	/	Better Corrosion inhibition	/		[19]
OX-CQDs, CQDs-C12H25, OX-CQDs-C12H25	CQDs (16.08%), CQDs-C12H25 (12.47%)	OX-CQDs (1.5nm)	OX-CQDs-C12H25 (10 $mg \cdot mL^{-1}$)	OX-CQDs-C12H25 (30.00 $mN \cdot m^{-1}$), CQDs-C12H25 (34.87 $mN \cdot m^{-1}$)	OX-CQDs-C12H25 (70.1°, 49.8°, 43.9°)	/	95%		[21]
CQDs, CQDs-C12H25	CQDs (23.49%), CQDs-C12H25 (3.54%)	/	OX-CQDs-C12H25 (0.7 $mg \cdot mL^{-1}$)	OX-CQDs-C12H25 (32.00 $mN \cdot m^{-1}$)	/	/	90%		[22]
CQDs-C12H25, OX-CQDs-C12H25, OX-CQDs-C14H29, OX-CQDs-C16H33	CQDs (6.09%), OX-CQDs (8.17%), OX-CQDs-C12H25	1.8-2.0nm	OX-CQDs-C12H25(10 $mg \cdot mL^{-1}$)	OX-CQDs-C12H25 (26.7 $mN \cdot m^{-1}$)	CQDs-C12H25 (75.5°, 50.1°, 44.6°), OX-CQDs-C12H25	/	100%		[23]

	(6.44%)				(70.4°, 43.4°, 38.0°)	
CQDs, NCQDs-12, NCQDs-14, NCQDs-16	5.7%	5nm	0.75	39.08	88.80	17.71
	6.7%		0.14	22.86	84.14	
	10.1%		0.1	28.88	64.26	
	14.5%	2.5-3nm	0.08	35.38	80.40	

Section I. Estimated average particle size of NCQDs

1.1 Moles of n-$C_{12}H_{25}Cl$

The molecular weight of n-$C_{12}H_{25}Cl$ is 204.8 g·mol^{-1}. Thus, 1 g of n-$C_{12}H_{25}Cl$ corresponds to 4.88 × 10^{-3} mol.

1.2 Estimation of the Equivalent Molar Amount of NCQDs

NCQDs do not have a precise molecular weight. Therefore, an equivalent molar amount was estimated by assuming spherical particles with an average diameter of 5 nm and a density of approximately 1.8 g·cm^{-3}, following common practice for carbon nanomaterials.

Parameter: $r=2.5\times10^{-7}$ cm

Single particle volume: $V=4\pi r^3/3=6.5\times10^{-20}$ cm^3

Single particle mass: $m=\rho V=1.17\times10^{-19}$ g

Number of particles in 1 g NCQDs: $N=8.5\times10^{18}$

Equivalent molar quantity: $n=N/N_A\approx1.4\times10^{-5}$ mol

1.3 Equivalent Molar Ratio

Based on the above estimation, the equivalent molar ratio of n-$C_{12}H_{25}Cl$ to NCQDs is approximately 350:1, indicating that the alkylating agent was used in excess to ensure efficient surface modification.

Section II. Deconvolution fitting parameters

Table S2 XPS atomic composition

Surfactant	C （%）	N （%）	O （%）	Quaternary fraction (%)
NCQDs	52.9	27.8	19.3	0
NCQDs-12	53.8	27.1	19.1	25
NCQDs-14	54.7	26.5	18.8	24
NCQDs-16	55.3	25.9	18.7	22

Table S3 Deconvolution fitting parameters of C 1s

	Peak	Binding energy	Area (%)

		(eV)	
NCQDs	C-C/C=C	284.8 eV	58
	C-O/C-N	286.2 eV	30
	C=O	288.6rV	12
NCQDs-12	C-C/C=C	284.8 eV	68
	C-O/C-N	286.2 eV	23
	C=O	288.6rV	9
NCQDs-14	C-C/C=C	284.8 eV	72
	C-O/C-N	286.2 eV	20
	C=O	288.6rV	8
NCQDs-16	C-C/C=C	284.8 eV	76
	C-O/C-N	286.2 eV	17
	C=O	288.6rV	7

Table S4 Deconvolution fitting parameters of N 1s

	Peak	Binding energy (eV)	Area (%)
NCQDs	Pyridinic N	398.14 eV	55.7
	Pyrrolic/amine N	399.80 eV	44.3
NCQDs-12	Pyridinic N	398.27 eV	49.8
	Pyrrolic/amine N	399.44 eV	24.5
	Quaternary N	400.78 eV	28.7
NCQDs-14	Pyridinic N	398.11 eV	61.0
	Pyrrolic/amine N	399.30 eV	18.6
	Quaternary N	400.72 eV	20.4
NCQDs-16	Pyridinic N	398.11 eV	57.2
	Pyrrolic/amine N	399.39 eV	20.7
	Quaternary N	400.85 eV	22.1

Table S5 Deconvolution fitting parameters of O 1s

	Peak	Binding energy (eV)	Area (%)
NCQDs	C-O	530.92	34.6
	C=O	529.99	65.4
NCQDs-12	C-O	531.04	41.2
	C=O	530.24	58.8

NCQDs-14	C-O	531.41	48.5
	C=O	529.97	51.5
NCQDs-16	C-O	531.18	45.1
	C=O	529.97	54.9

Section III. Calculation of Quantum Yield

The absolute fluorescence quantum yields of the prepared NCQDs and NCQDs-n were determined using a comparative method with quinine sulfate as the reference.

3.1 Sample Preparation

The samples were diluted to ensure that the optical density (OD) at the excitation wavelength did not exceed 0.1 to minimize inner filter effects. Quinine sulfate was prepared at a comparable OD under the same conditions. Fluorescence emission spectra of both the sample and the reference were recorded using a fluorescence spectrometer with excitation wavelengths selected according to the maximum absorption of each sample. All measurements were corrected for the spectral response of the instrument.

3.2 Quantum Yield Calculation

The relative quantum yield was calculated using the following equation:

$$\Phi_{sample} = \Phi_{ref} \cdot \frac{I_{sample}}{I_{ref}} \cdot \frac{I_{ref}}{I_{sample}} \cdot \left(\frac{n_{sample}}{n_{ref}}\right)^2$$

where:

Φ_{sample} and Φ_{ref} are the quantum yields of the sample and reference, respectively.

I_{sample} and I_{ref} are the integrated fluorescence intensities.

A_{sample} and A_{ref} are the absorbances at the excitation wavelength.

n_{sample} and n_{ref} are the refractive indices of the solvents used for the sample and reference, respectively.

3.3 Reproducibility

All measurements were repeated three times, and the reported quantum yields represent the average values with standard deviations.

Section IV.

a) Mobility ratio

$$M = \frac{\lambda_{\text{displacing}}}{\lambda_{\text{displaced}}} = \frac{k_{rw}/\mu_w}{k_{ro}/\mu_o}$$

k_{rw} and k_{ro} represent the relative permeability of water and oil phase, respectively;

μ_w and μ_o donate the viscosity of water and oil phase, respectively.

b) Residue resistance factor, R_f

$$R_f = \frac{k_{w,\,before}}{k_{w,\,after}}$$

$k_{w,\,before}$ is water phase permeability before water injection;

$k_{w,\,after}$ is water phase permeability after injecting displacement fluid.

Section V.

Table S6 Interfacial tension data vs salinity.

	NCQDs	NCQDs-12	NCQDs-14	NCQDs-16
0	2.24351	0.74495	0.05161	0.01934
1	2.20205	0.57581	0.02757	0.01114
3	1.28904	0.36236	0.01997	0.00601
5	1.08851	0.31371	0.01728	0.00502
7	0.92605	0.28629	0.01547	0.00422
10	0.40525	0.11131	0.01408	0.00445

Table S7 Surface tension data.

Mass concentration ($mg \cdot L^{-1}$)	NCQDs	NCQDs-12	NCQDs-14	NCQDs-16
1E-3	70.96	70.38	71.92	71.58
0.005	68.53	66.19	57.29	62.79
0.01	66.63	57.06	50.79	59.92
0.025	65.81	45.62	43.09	49.25
0.05	58.93	35.16	35.39	41.55
0.075	55.03	30.87	32.34	35.49
0.1	52.88	28.2	28.88	34.94
0.2	46.12	26.14	27.57	32.52

	0.5	40.76	26.35	27.25	31.09
	1	38.93			
	2	38.63			

Table S8 Coreflood oil production data.

Injected volume (PV)	1231		NCQDs-14	
	Injected pressure (MPa)	Oil recovery (%)	Injected pressure (MPa)	Oil recovery (%)
0	0.05	0	0.09	0
1	0.21	1.71	0.28	3.43
2	0.53	4.1	0.62	7.14
3	0.89	8.53	1.01	14.57
4	1.27	17.41	1.84	23.43
5	1.82	27.99	2.52	33.14
6	2.31	39.59	3.04	44.29
7	2.64	52.9	3.29	50.86
8	2.89	54.95	3.47	57.14
9	3.12	56.31	3.52	58.57
10	3.24	57	3.58	59.14
11	3.26	57.34	3.61	59.43
12	3.29	57.68	3.65	59.71
13	3.3	58.02	3.69	60
14	3.31	58.02	3.72	60
15	3.31	58.02	3.72	60
16	3.27	58.02	3.72	60
16.5	3.21	58.36	3.67	60.29
17	3.15	59.04	3.61	61.43
17.5	3.13	60.07	3.49	68
18	3.11	61.43	3.43	72.57
18.5	3.1	62.12	3.37	74.57
19	3.09	62.46	3.32	74.86
19.5	3.09	62.8	3.31	74.86
20	3.09	63.14	3.3	74.86
21	3.08	63.14	3.3	75.14
22	3.06	63.48	3.28	75.71
23	3.05	63.82	3.26	76.57
24	3.04	64.16	3.2	77.14

25	3.03	64.16	3.14	77.43
26	3.02	64.51	3.12	77.71
27	3.01	64.51	3.11	77.71
28	2.99	64.51	3.11	77.71
29	2.99	64.51	3.11	77.71
30	2.99	64.51	3.11	77.71

Figure S1 Figure of contact angle.

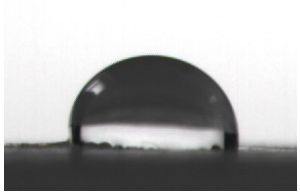

Primitive

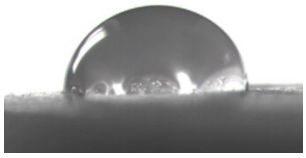

NCQDs

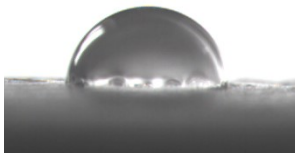

NCQDs-12

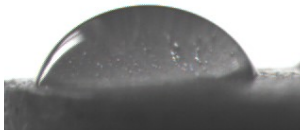

NCQDs-14

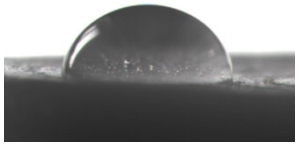

NCQDs-16